Soil chemistry determines whether defensive plant secondary metabolites promote or suppress herbivore growth

Lingfei Hu[a,b], Zhenwei Wu[a], Christelle A. M. Robert[b], Xiao Ouyang[a], Tobias Züst[b,1], Adrien Mestrot[c], Jianming Xu[a,2], and Matthias Erb[b,2]

[a]Institute of Soil and Water Resources and Environmental Science, College of Environmental and Resource Sciences, Zhejiang Provincial Key Laboratory of Agricultural Resources and Environment, Zhejiang University, Hangzhou 310058, China; [b]Institute of Plant Sciences, University of Bern, 3013 Bern, Switzerland; and [c]Institute of Geography, University of Bern, 3012 Bern, Switzerland

Edited by James H. Tumlinson, Pennsylvania State University, University Park, PA, and approved September 10, 2021 (received for review May 24, 2021)

Plant secondary (or specialized) metabolites mediate important interactions in both the rhizosphere and the phyllosphere. If and how such compartmentalized functions interact to determine plant–environment interactions is not well understood. Here, we investigated how the dual role of maize benzoxazinoids as leaf defenses and root siderophores shapes the interaction between maize and a major global insect pest, the fall armyworm. We find that benzoxazinoids suppress fall armyworm growth when plants are grown in soils with very low available iron but enhance growth in soils with higher available iron. Manipulation experiments confirm that benzoxazinoids suppress herbivore growth under iron-deficient conditions and in the presence of chelated iron but enhance herbivore growth in the presence of free iron in the growth medium. This reversal of the protective effect of benzoxazinoids is not associated with major changes in plant primary metabolism. Plant defense activation is modulated by the interplay between soil iron and benzoxazinoids but does not explain fall armyworm performance. Instead, increased iron supply to the fall armyworm by benzoxazinoids in the presence of free iron enhances larval performance. This work identifies soil chemistry as a decisive factor for the impact of plant secondary metabolites on herbivore growth. It also demonstrates how the multifunctionality of plant secondary metabolites drives interactions between abiotic and biotic factors, with potential consequences for plant resistance in variable environments.

plant secondary metabolites | benzoxazinoids | herbivore resistance | plant herbivore interactions | maize

Organismal traits are commonly coopted for multiple functions (1–4). In complex and fluctuating environments, multifunctionality may lead to fitness trade-offs with important consequences for ecological and evolutionary dynamics (5–7).

Plant secondary (or specialized) metabolites are important mediators of species interactions in natural and agricultural systems (8). Many plant secondary metabolites have been documented to protect plants against insect herbivores by acting as toxins, digestibility reducers, and/or repellents (9). Plant secondary metabolites also serve other functions: they can, for instance, act as signaling molecules (10), photoprotectants (11), antibiotics (12), soil nutrient mobilizers (13), and precursors of primary metabolites (14). Recent genetic work has highlighted that the same plant secondary metabolites may engage in multiple functions (4, 15, 16), leading to potentially important interactions between different environmental factors (6, 17). How this multifunctionality influences plant ecology and plant–insect interactions in complex environments is not well understood.

The soil environment can have a major impact on plant defense expression and plant–herbivore interactions. Soil nutrients and micronutrients can reprogram plant defenses through cross talk between defense and nutrient signaling (18, 19) or by influencing soil microbes, which subsequently modulate plant defense responses (20, 21). Elements such as silicon (Si) can also act as defenses directly by forming crystals on the leaf surface (22). In addition, soil nutrients can also influence plant–herbivore interactions by changing the nutritional value of the plant to herbivores (23). Thus, plant secondary metabolites with dual functions in the rhizosphere and phyllosphere may mediate interactions between soil chemistry and herbivores (24).

Benzoxazinoids are shikimic acid–derived secondary metabolites that are produced in high abundance by grasses such as wheat and maize. They evolved multiple times within the plant kingdom and are also found in various dicot families (25). Initially, benzoxazinoids were described as defense compounds that suppress and repel insect herbivores (26). Later genetic work revealed that benzoxazinoids also act as within-plant signaling compounds by initiating callose deposition upon pathogen and aphid attack (27, 28). Benzoxazinoids are also released into the rhizosphere in substantial quantities (29), where they can chelate iron (30), thus making it bioavailable (31). By

Significance

This study demonstrates that the protective effects of multifunctional maize secondary metabolites against a major pest are dependent on soil chemical composition. By functioning as both digestibility reducers and siderophores, benzoxazinoids link soil chemistry to plant–environment interactions. Given that many plant secondary metabolites have multiple functions in roots and leaves, such links are likely widespread and may govern community composition and pest dynamics across different (agro)ecosystems. The presented findings also illustrate the limits and context dependency of using multifunctional plant secondary metabolites to combat major herbivore pests. The latter is particularly important in the context of the threat that the fall armyworm poses for global maize production.

Author contributions: L.H., C.A.M.R., J.X., and M.E. designed research; L.H., Z.W., X.O., and T.Z. performed research; J.X. and M.E. contributed new reagents/analytic tools; L.H., C.A.M.R., A.M., J.X., and M.E. analyzed data; and L.H., C.A.M.R., and M.E. wrote the paper.

The authors declare no competing interest.

This article is a PNAS Direct Submission.

[1]Present address: Institute for Systematic and Evolutionary Botany, University of Zürich, 8008 Zürich, Switzerland.

[2]To whom correspondence may be addressed. Email: jmxu@zju.edu.cn or matthias.erb@ips.unibe.ch.

This article contains supporting information online at http://www.pnas.org/lookup/suppl/doi:10.1073/pnas.2109602118/-/DCSupplemental.

Published October 21, 2021.

consequence, benzoxazinoids can influence plant iron homeostasis. Recently, a link was documented between the iron chelating capacity and the interaction between maize plants and the western corn rootworm. This highly adapted insect is attracted by iron benzoxazinoid complexes and can use them for its own iron supply (31). Thus, it is conceivable that the multiple functions of benzoxazinoids may lead to trade-offs between their function as defenses and their functions as providers of essential micronutrients.

Here, we explore how the multifunctionality of benzoxazinoids shapes interactions between soil conditions and a leaf herbivore. By comparing soils that differ in their trace element composition, we uncover that the protective effect of maize benzoxazinoids against the fall armyworm can be reversed to a susceptibility effect in certain soils. Using micronutrient analyses and manipulative laboratory experiments, we document that this phenomenon can be explained by the interaction of benzoxazinoids with free iron in the soil. We further document that iron and benzoxazinoids interact to control leaf defenses but that the benzoxazinoid-dependent susceptibility is best explained by increased iron supply to the fall armyworm. Taken together, these results provide a mechanistic link between soil properties and leaf–herbivore interactions and illustrate how plant secondary metabolite multifunctionality shapes plant–herbivore interactions.

Results

The Effect of Benzoxazinoids on Herbivore Performance Depends on Soil Type. Benzoxazinoids increase leaf resistance to herbivores but also interact with soil micronutrients and microbial communities in the soil (31–33). To test whether the defensive function of benzoxazinoids is modulated by soil properties, we collected soils from eight different arable fields around Yixing (Jiangsu province, China), including anthrosols with expected high availability of free iron and ferrosols with expected low availability of iron (classification according to Chinese soil taxonomy, refer to *SI Appendix*, Fig. S1 and Table S1 for basic soil characteristics). We then grew wild-type B73 (WT) and benzoxazinoid-deficient *bx1* mutant plants in the different soils, infected the plants with fall armyworm larvae, and measured plant performance, leaf damage, and larval performance. On plants grown in ferrosols, fall armyworm larvae gained more weight on *bx1* mutant plants than WT plants, as expected from the defensive function of benzoxazinoids (Fig. 1). However, on plants grown in anthrosols, the larvae gained more weight on WT plants than *bx1* mutant plants (Fig. 1). Leaf damage did not differ between genotypes (*SI Appendix*, Fig. S2*A*), implying a change in the digestibility of the consumed leaf material. Overall, maize seedlings accumulated more biomass when growing in anthrosols than ferrosols, with no differences between genotypes (*SI Appendix*, Fig. S2*B*). To confirm that the herbivore growth patterns depend on benzoxazinoid biosynthesis, we tested additional *bx1* and *bx2* mutant alleles in the W22 background in an anthrosol and a ferrosol. Again, the larvae grew better on *bx1* and *bx2* mutants in the ferrosol but grew significantly less on the mutants in the anthrosol (*SI Appendix*, Fig. S3). Thus, the impact of benzoxazinoid biosynthesis on herbivore performance is strongly dependent on the soil type.

Soil-Dependent Benzoxazinoid Resistance Is Driven by Root Iron Supply. Benzoxazinoids can chelate micronutrients and trace metals (30, 34), with the strongest quenching being observed for iron (31). We thus explored correlations between different soil properties and available micronutrients and the *bx1*-dependent impact on fall armyworm performance. Principal component analysis (PCA) resulted in a clear separation of anthrosols from ferrosols (Fig. 1*I*). Ferrosols, on which larvae grew better on *bx1* than WT plants, had a slightly higher pH, less organic carbon, very low bioavailable iron, copper, boron, and phosphorus but higher sodium, magnesium, and silicon than anthrosols (Fig. 1*I* and *SI Appendix*, Fig. S1). To further narrow down potential micronutrients that may drive the different genotype-specific performance of the fall armyworm, we screened micronutrient levels in the leaves of WT and *bx1* plants growing in the different soils. ANOVA revealed significant genotype effects for calcium and iron, with overall higher levels of both elements in the leaves of WT than *bx1* mutant plants (*SI Appendix*, Fig. S4). Furthermore, a significant interaction between genotype and soil type was found for iron (Fig. 1*J*), with higher iron levels in WT plants than *bx1* mutant plants in anthrosols with high available iron and no difference in ferrosols with very low available iron (Fig. 1*J*). Overall iron levels were enhanced in plants grown in anthrosols compared to plants grown in ferrosols (Fig. 1*J*), which is expected, given that iron in ferrosols is chiefly present as insoluble iron oxide. Quantitative analyses revealed a strong association between higher iron levels in WT plants and higher fall armyworm performance (*SI Appendix*, Fig. S5). An association was also observed for copper (*SI Appendix*, Fig. S5), but this pattern was not associated with significant differences in copper levels between genotypes (*SI Appendix*, Fig. S5). No correlation was observed for calcium (*SI Appendix*, Fig. S5). The association between plant iron and fall armyworm performance was conserved in the W22 background (*SI Appendix*, Fig. S6).

Based on these results, we hypothesized that differences in iron availability may determine the impact of benzoxazinoids on herbivore performance. To test this hypothesis, we grew WT and *bx1* mutant plants in nutrient solutions with different forms of iron (31). Plants where either grown in iron-deficient solutions (supplemented with NaCl or Na_2SO_4), solutions containing free, soluble iron [supplied as $FeCl_3$ or $Fe_2(SO_4)_3$] that requires chelation by siderophores for efficient uptake, or solutions containing a bioavailable iron complex Fe–ethylenediaminetetraacetic acid (Fe-EDTA). Fall armyworm larvae grew better on benzoxazinoid-deficient *bx1* mutant plants than WT plants in iron-free and Fe-EDTA nutrient solutions but worse on *bx1* mutant plants than WT plants in solutions containing free iron (Fig. 2*A* and *SI Appendix*, Fig. S7). Leaf damage was similar across genotypes and iron treatments (Fig. 2*B*). Complementation of *bx1* mutant plants with pure 2,4-dihydroxy-7-methoxy-1,4-benzoxazin-3-one (DIMBOA, 300 μg) added to the rhizosphere reverted the *bx1* phenotype in solutions containing free iron (Fig. 2*C*). These results show that the interaction between benzoxazinoids and iron availability can modulate the impact of benzoxazinoids on leaf herbivore performance.

Interactions between Root Iron Supply and Benzoxazinoids Determine Leaf Iron Homeostasis. *Bx1* mutant plants at the seedling stage are less efficient at taking up free iron than WT plants due to the absence of DIMBOA in the rhizosphere of *bx1* mutants (31). Thus, iron supply and benzoxazinoids likely interact to determine leaf iron homeostasis. In support of this hypothesis, we find that WT plants contain more iron in their leaves than *bx1* plants when grown in soils in which iron is available in free or weakly complexed form but not in soil in which iron availability is low (Fig. 1 and *SI Appendix*, Figs. S4 and S7). To further explore this aspect, we measured the expression of genes involved in iron homeostasis in the leaves of WT and *bx1* mutant plants grown under different forms of iron supply (Fig. 3 and *SI Appendix*, Fig. S8). The tested genes included genes associated with iron transport, such as *ZmYS1*, *ZmNRAMP1*, and *ZmIRO2*, and genes that are likely involved in the biosynthesis and efflux of the mugineic acid family of siderophores, such as *ZmRP1*, *ZmIDI4*, *ZmNAS3*, *ZmDMAS1*, and *ZmTOM2* (35–37). We found strong interactions between iron availability and the *bx1* mutation for seven of the eight

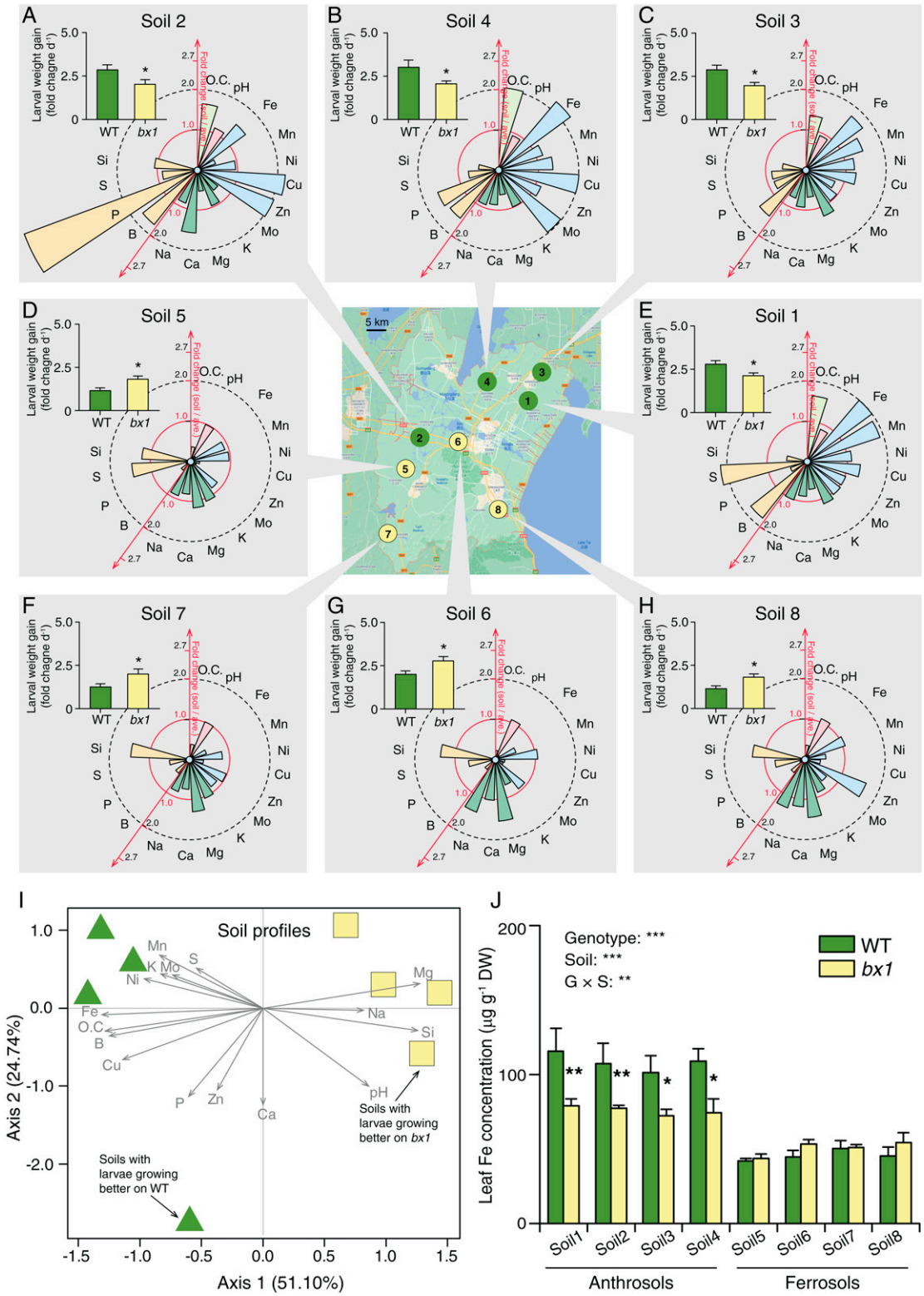

Fig. 1. The effect of benzoxazinoids on herbivore performance depends on the soil type. (*Center*) Map depicting soil collection sites around Yixing (China). Gray boxes (*A–H*): Growth of *S. frugiperda* caterpillars on WT and benzoxazinoid-deficient *bx1* mutant plants growing in the different soils (+SE, $n = 10$), together with respective soil properties. Soil properties are depicted as fold change relative to the average across all tested soils. Refer to *SI Appendix*, Fig. S1 for absolute values. Soils 1 through 4 are anthrosols, and soils 5 through 8 are ferrosols. Asterisks indicate significant differences between plant genotypes (ANOVA; $*P < 0.05$). (*I*) PCA of field soil properties. Green triangles represent soils on which caterpillars grow better on WT plants. Yellow squares represent soils on which caterpillars grow better on *bx1* mutant plants. Vectors of soil parameters are shown as gray arrows. (*J*) Iron contents in the leaves of WT and *bx1* plants grown in the different soils (+SE, $n = 3$, with three to four individual plants pooled per replicate). For full elemental analysis, refer to *SI Appendix*, Fig. S4. DW, dry weight. O.C., organic carbon. Two-way ANOVA results testing for genotype and soil effects are shown ($**P < 0.01$; $***P < 0.001$). Asterisks indicate significant differences between genotypes within the same soil (pairwise comparisons through FDR-corrected LSMeans; $*P < 0.05$; $**P < 0.01$).

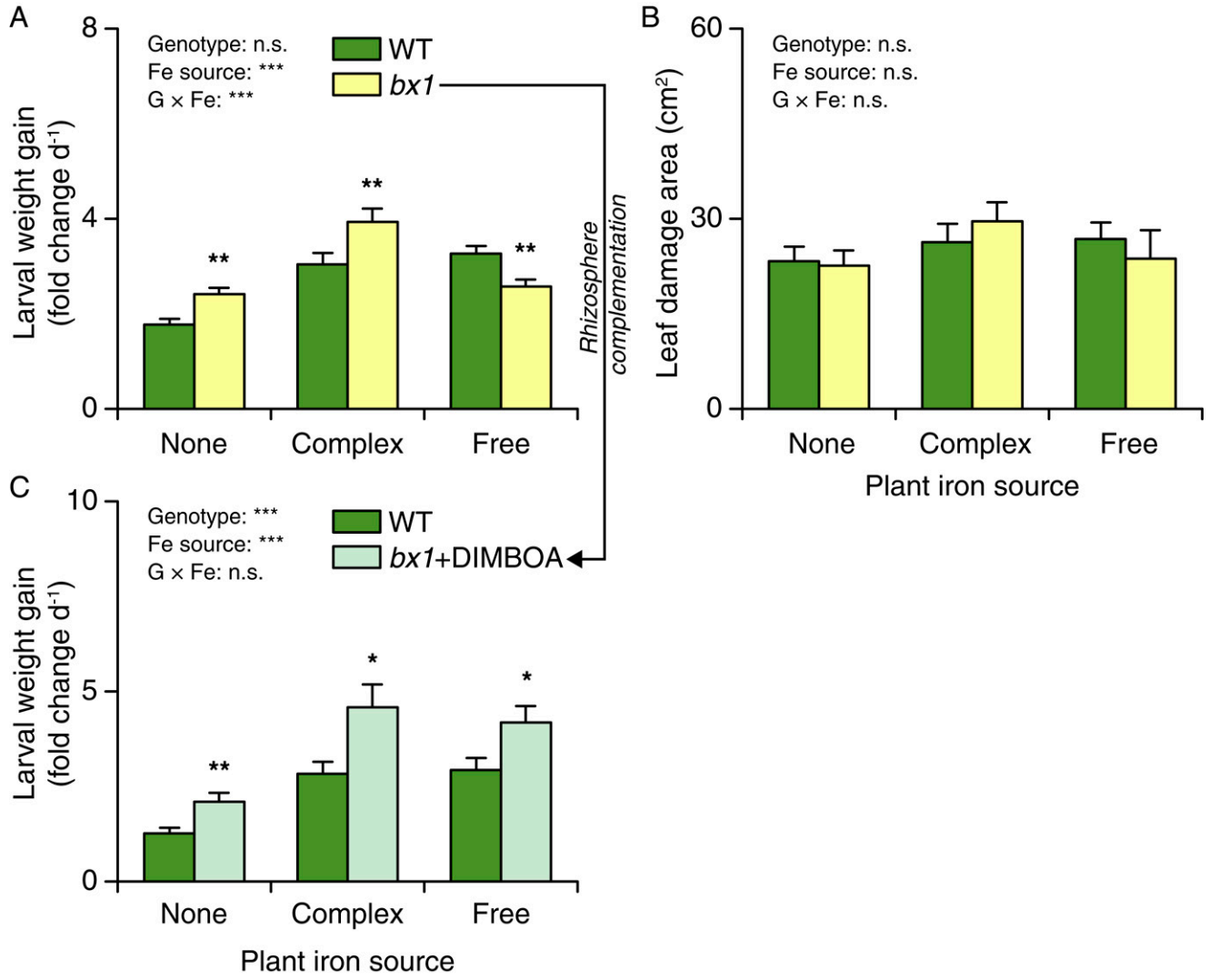

Fig. 2. Soil-dependent benzoxazinoid resistance is driven by root iron supply. (*A*) Growth of *S. frugiperda* feeding on WT and *bx1* plants supplied with different iron sources (+SE, $n = 14$ to 15). (*B*) Consumed leaf area (+SE, $n = 14$ to 15). (*C*) Growth of *S. frugiperda* feeding on WT and *bx1* plants complemented with pure DIMBOA added to the rhizosphere under different iron sources (+SE, $n = 14$ to 15). "None" nutrient solutions received either NaCl or Na_2SO_4. "Complex" nutrient solutions received Fe-EDTA. "Free" nutrient solutions received $FeCl_3$ or $Fe_2(SO_4)_3$. For full results showing genotype effects of all individual nutrient solutions, refer to *SI Appendix*, Fig. S7. Two-way ANOVA results testing for genotype and iron source effects are shown (n.s., not significant; $***P < 0.001$). Asterisks indicate significant differences between genotypes within the same soil (pairwise comparisons through FDR-corrected LSMeans; $*P < 0.05$; $**P < 0.01$).

tested genes. Most iron homeostasis genes were highly expressed under iron-deficient conditions and suppressed in the presence of complex iron, with no differences between WT and *bx1* mutant plants. When iron was present in its free form, most of these genes were strongly induced in the *bx1* mutant but not in WT plants (Fig. 3). Exceptions to this pattern included *ZmNAS3*, which showed opposite expression patterns, and *ZmTOM2*, whose expression was not modulated by the *bx1* mutation (Fig. 3). These results show that root iron supply strongly modulates leaf iron homeostasis, with *bx1* mutants exhibiting iron-deficiency gene expression patterns when grown in the presence of free iron.

Changes in Leaf Herbivore Performance Are Not Explained by Changes in Leaf Primary Metabolism and Defense Expression. How can soil- and benzoxazinoid-dependent leaf iron homeostasis explain fall armyworm performance? In theory, iron homeostasis may indirectly affect leaf quality by changing leaf primary metabolism and defense expression (38–40) or directly by acting as a herbivore micronutrient (23). To test the first hypothesis, we measured soluble protein, hydrolysable amino acid, and carbohydrate levels in the leaves of WT and *bx1* mutant plants grown under different iron regimes (Fig. 4 and *SI Appendix*, Fig. S9). No significant differences were found, suggesting that the different performance of the fall armyworm is not explained by major changes in leaf primary metabolites.

Next, we measured the production of leaf defense metabolites that are produced independently of the benzoxazinoid biosynthesis pathway, including chlorogenic acid, rutin, and maysin, which have been associated with fall armyworm resistance in vitro and through correlative approaches (41–43), and the expression of defense marker genes, including a proteinase inhibitor (*ZmMPI*) (44) and a gene encoding the defense protein RIP2 (*ZmRIP2*), which is toxic to the fall armyworm in vitro (45). We detected significant interactions between iron availability and the *bx1* mutation for rutin and *ZmRIP2*

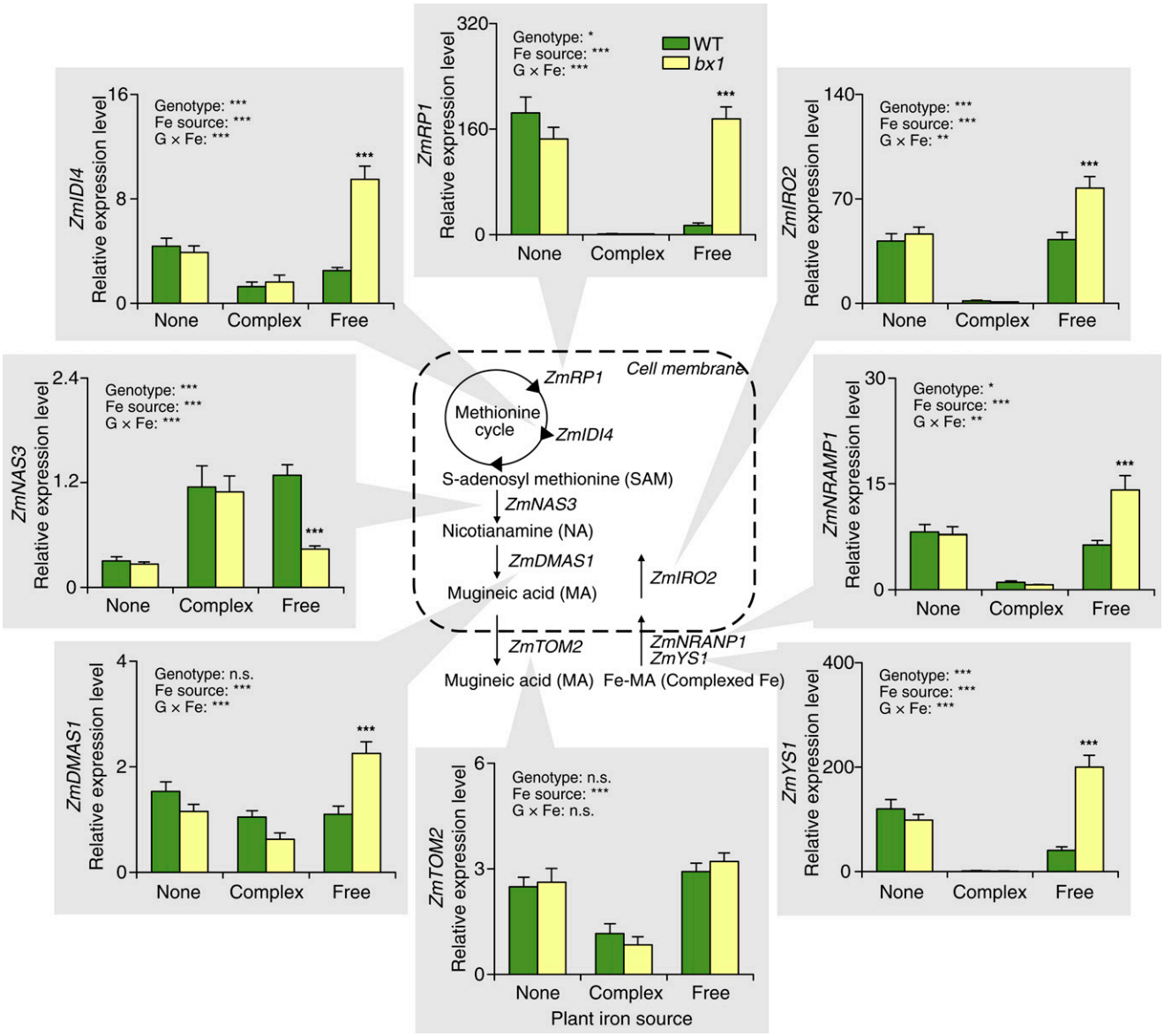

Fig. 3. Interactions between root iron supply and benzoxazinoids determine leaf iron homeostasis. Relative expression of genes involved in iron homeostasis in the leaves of WT and *bx1* mutant plants supplied with different iron sources (+SE, $n = 7$ to 8). "None" nutrient solutions received either NaCl or Na_2SO_4. "Complex" nutrient solutions received Fe-EDTA. "Free" nutrient solutions received $FeCl_3$ or $Fe_2(SO_4)_3$. For full results showing genotype effects of all individual nutrient solutions, refer to *SI Appendix*, Fig. S8. Two-way ANOVA results testing for genotype and iron source effects are shown (n.s., not significant; $*P < 0.05$; $**P < 0.01$; $***P < 0.001$). Asterisks indicate significant differences between genotypes within the same soil (pairwise comparisons through FDR-corrected LSMeans; $***P < 0.001$).

expression (Fig. 5 and *SI Appendix*, Fig. S10). More rutin was produced in *bx1* mutant plants than WT plants grown in the presence of complex iron but not when grown in iron-deficient and free-iron solutions. *ZmRIP2* expression was lower in the *bx1* mutant than in WT plants, and these effects were most pronounced when plants were grown in iron-deficient and free-iron solutions. These results show that root iron supply and benzoxazinoid biosynthesis interact to determine leaf-defense expression. At the same time, these interactions are unlikely to explain the observed differences in fall armyworm performance, as patterns do not match. *ZmRIP2* expression, for instance, was strongly reduced in the *bx1* mutant growing without iron or with iron in its free form, while fall armyworm performance was enhanced on *bx1* mutant plants grown without iron but suppressed in *bx1* plants grown with free iron.

Herbivore Iron Supply Is Associated with Soil-Dependent Benzoxazinoid Resistance. To test the hypothesis that benzoxazinoids may improve fall armyworm performance by supplying dietary iron, we first screened micronutrient concentrations in fall armyworm larvae fed on WT and *bx1* mutant plants grown in the different field soils. We found higher levels of iron in larvae feeding on WT than *bx1* mutant plants in soil with high iron availability. In soils with low iron availability, larval iron levels were low and not different between plant genotypes (Fig. 6*A*). No significant effects were found for the other tested elements (*SI Appendix*, Fig. S11). The same pattern for iron was observed for *bx1* and *bx2* mutants in the W22 genetic background (*SI Appendix*, Fig. S12). Larvae feeding on plants growing in different iron solutions showed corresponding patterns, with significantly lower larval iron levels when feeding on *bx1* than WT plants grown together

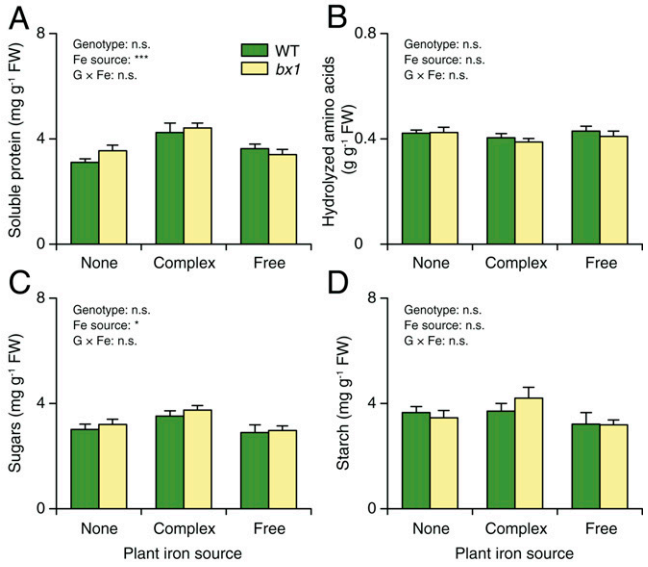

Fig. 4. Changes in leaf herbivore performance are not explained by changes in leaf primary metabolism. Contents of soluble protein (*A*), hydrolysable amino acids (*B*), sugars (*C*), and starch (*D*) in the leaves of WT and *bx1* mutant plants supplied with different iron sources (+SE, $n = 14$ to 15). "None" nutrient solutions received either NaCl or Na_2SO_4. "Complex" nutrient solutions received Fe-EDTA. "Free" nutrient solutions received $FeCl_3$ or $Fe_2(SO_4)_3$. For full results showing genotype effects of all individual nutrient solutions, refer to *SI Appendix*, Fig. S9. Two-way ANOVA results testing for genotype and iron source effects are shown (n.s., not significant; $*P < 0.05$; $***P < 0.001$). No significant differences between genotypes within the same soil were observed (pairwise comparisons through FDR-corrected LSMeans).

with free iron (Fig. 6*B* and *SI Appendix*, Fig. S13). Adding DIMBOA to the rhizosphere of *bx1* mutant plants restored larval iron levels (Fig. 6*C*), thus providing a direct link between benzoxazinoids in the rhizosphere and larval iron homeostasis. To test whether fall armyworm performance is affected by iron supply, we measured larval growth in the iron transport deficient *ys1* mutant (35, 46). Larvae gained less weight in the *ys1* mutant compared to B73 plants (Fig. 6*D*). As the genetic background of the *ys1* is not controlled, other genetic differences may also have influenced fall armyworm growth. Thus, we conducted iron supplementation experiments by producing an iron-deficient diet and supplementing it with different forms of iron, including the DIMBOA iron complex $Fe(III)(DIMBOA)_3$ at physiological concentrations. Fall armyworm larvae gained more weight when fed on iron supplemented diets, irrespective of the iron source (Fig. 6*E*). At the tested concentration, DIMBOA alone had no negative effect on fall armyworm growth, which is in accordance with earlier results (32). From these experiments, we conclude that the interaction between soil micronutrient composition and benzoxazinoid biosynthesis directly influences iron homeostasis of a leaf herbivore and that these effects can explain the soil-dependent impact of benzoxazinoids on herbivore performance.

Discussion

Organismal traits are commonly coopted for multiple functions, which can lead to important context-dependent performance patterns (5, 47). Here, we demonstrate that the multifunctionality of plant secondary metabolites results in conditional outcomes of plant–herbivore interactions, with soil properties determining whether the secondary metabolites promote or suppress leaf herbivore growth. We discuss the mechanisms and agroecological implications of this finding.

Multifunctionality is a common property of plant secondary metabolites (16, 48, 49), with potentially important consequences for organismal interactions. We find that the protective effect of benzoxazinoids against an herbivore is determined and fully reversible by specific soil properties. A series of manipulative experiments in combination with the current state of knowledge (48, 50) allows us to infer the following scenario. When ingested by herbivores, such as the fall armyworm, benzoxazinoids are rapidly deglycosylated (32). While the more stable forms, such as DIMBOA, can be detoxified through stereoselective reglycosylation (51), less stable aglucones, such as HDMBOA, can form reactive hemiacetals that form covalent bonds with thiol groups and can thus act as digestibility reducers as well as behavioral modulators (32, 52). These effects likely contribute to reduced herbivore weight gain of the fall armyworm in the presence of benzoxazinoids. At the same time, however, benzoxazinoids are also released into the rhizosphere, where they interact with soil microbes (53) and effectively chelate free (31) and weakly bound iron, thus making it available to the plant. The higher iron uptake increases leaf iron levels, which benefits herbivores whose growth is limited by iron supply. The net impact of benzoxazinoid biosynthesis on the interaction between maize and leaf herbivores is thus likely governed by the strength of the negative effects of benzoxazinoids as digestibility reducers and the strength of the positive effects of benzoxazinoids as siderophores. By consequence, soil chemistry can tip the balance and determine whether benzoxazinoids have a net positive or negative effect on herbivore performance.

Plant nutrients in general (19, 22, 54–57) and soil iron supply in particular (20, 21, 58), are increasingly recognized as important modulators of plant defense expression. In *Arabidopsis thaliana*, for instance, the coumarin scopoletin is secreted under iron deficiency and influences root microbiome assembly (21), likely including microbes that subsequently trigger systemic resistance in the plant by activating or priming hormonal defense pathways (20). Another example is Si in the soil, which can modulate plant nitrogen supply (59) and can also be used directly by plants to form defensive crystals on leaf surfaces (60), thus resulting in significant interactive effects of soil nitrogen and silicon on herbivore performance (61). In our work, we find that benzoxazinoid biosynthesis interacts with root iron supply to regulate a subset of leaf defenses, including the phenolic acid rutin and messenger RNA levels of the defense protein ZmRIP2. These effects are unlikely to be caused by changes in primary metabolism via leaf iron supply, as leaf carbohydrates and amino acids do not show any differences between treatments at this growth stage. Interestingly, patterns of defense expression and leaf iron homeostasis markers also do not correspond: While iron homeostasis is most strongly affected by benzoxazinoids in the presence of free iron, defense expression is most strongly affected by the presence of the iron complex Fe-EDTA in the growth medium. Benzoxazinoids shape the rhizosphere microbiome (53, 62, 63), and this effect may be modulated by competition for iron. It is thus possible that the type of iron source that is present in the growth solution has an impact on benzoxazinoid–microbiome interactions, which, again, may affect the activation of leaf defenses through systemic signaling. Further experiments will be required to explore this hypothesis. Although the observed modulation of the measured leaf defense metabolites and defense genes may have contributed to fall armyworm growth, they are not directly responsible for the observed benzoxazinoid-dependent patterns, as benzoxazinoids affect fall armyworm growth differently in no-iron and free-iron treatments, without any change in benzoxazinoid-mediated defense expression. It should be

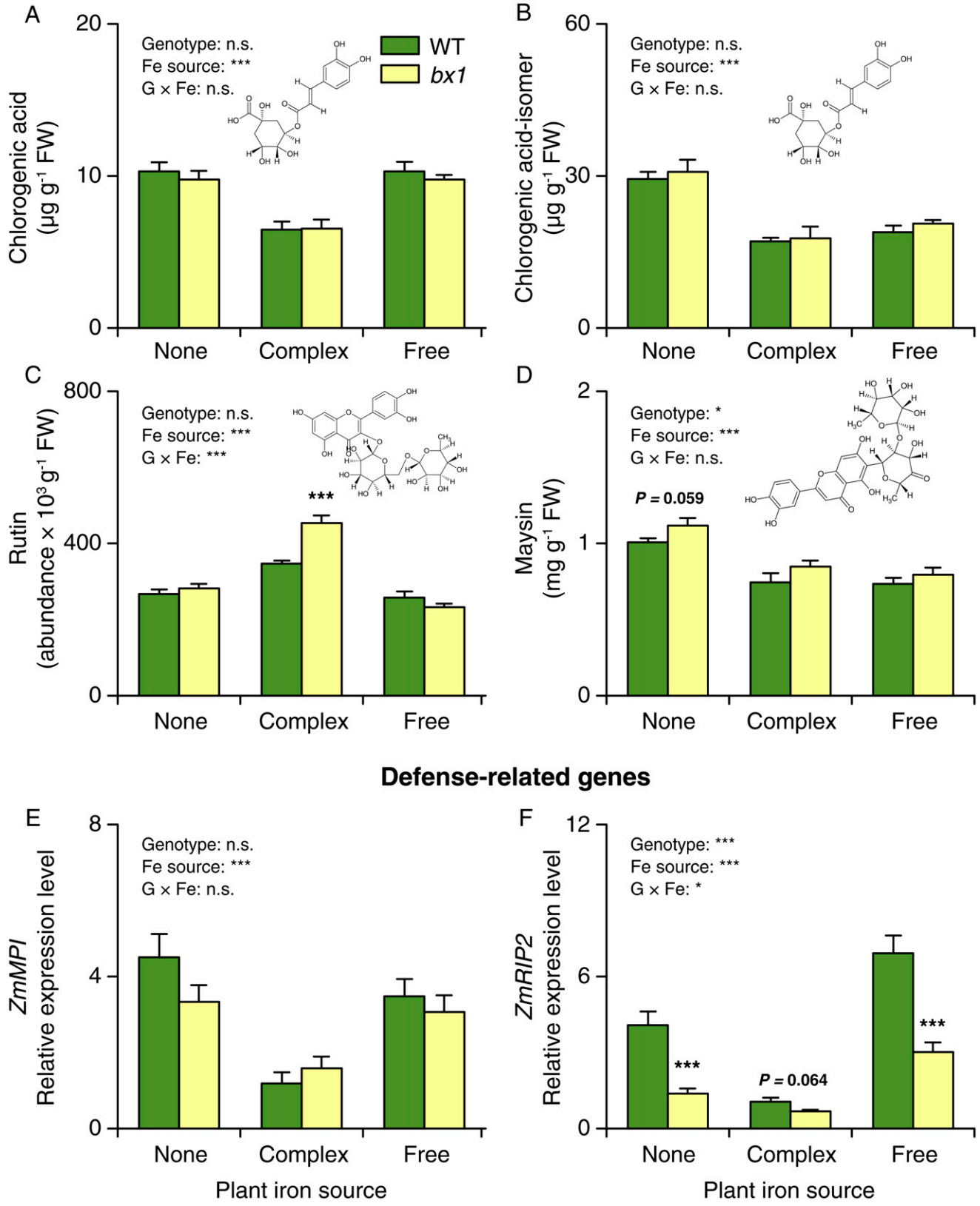

Fig. 5. Soil iron and benzoxazinoids interactively reprogram a subset of leaf defenses. (*A–D*) Concentrations of chlorogenic acid (*A*), chlorogenic acid isomer (*B*), rutin (*C*), and maysin (*D*) in the leaves of WT and *bx1* mutant plants supplied with different iron sources (+SE, $n = 8$). FW, fresh weight. (*E* and *F*) Expression levels of *ZmMPI* (*E*) and *ZmRIP2* (*F*) in the leaves of WT and *bx1* plants supplied with different iron sources (+SE, $n = 8$). "None" nutrient solutions received either NaCl or Na_2SO_4. "Complex" nutrient solutions received Fe-EDTA. "Free" nutrient solutions received $FeCl_3$ or $Fe_2(SO_4)_3$. For full results showing genotype effects of all individual nutrient solutions, refer to *SI Appendix*, Fig. S10. Two-way ANOVA results testing for genotype and iron source effects are shown (*$P < 0.05$; ***$P < 0.001$). Asterisks indicate significant differences between genotypes within the same soil (pairwise comparisons through FDR-corrected LSMeans; ***$P < 0.001$).

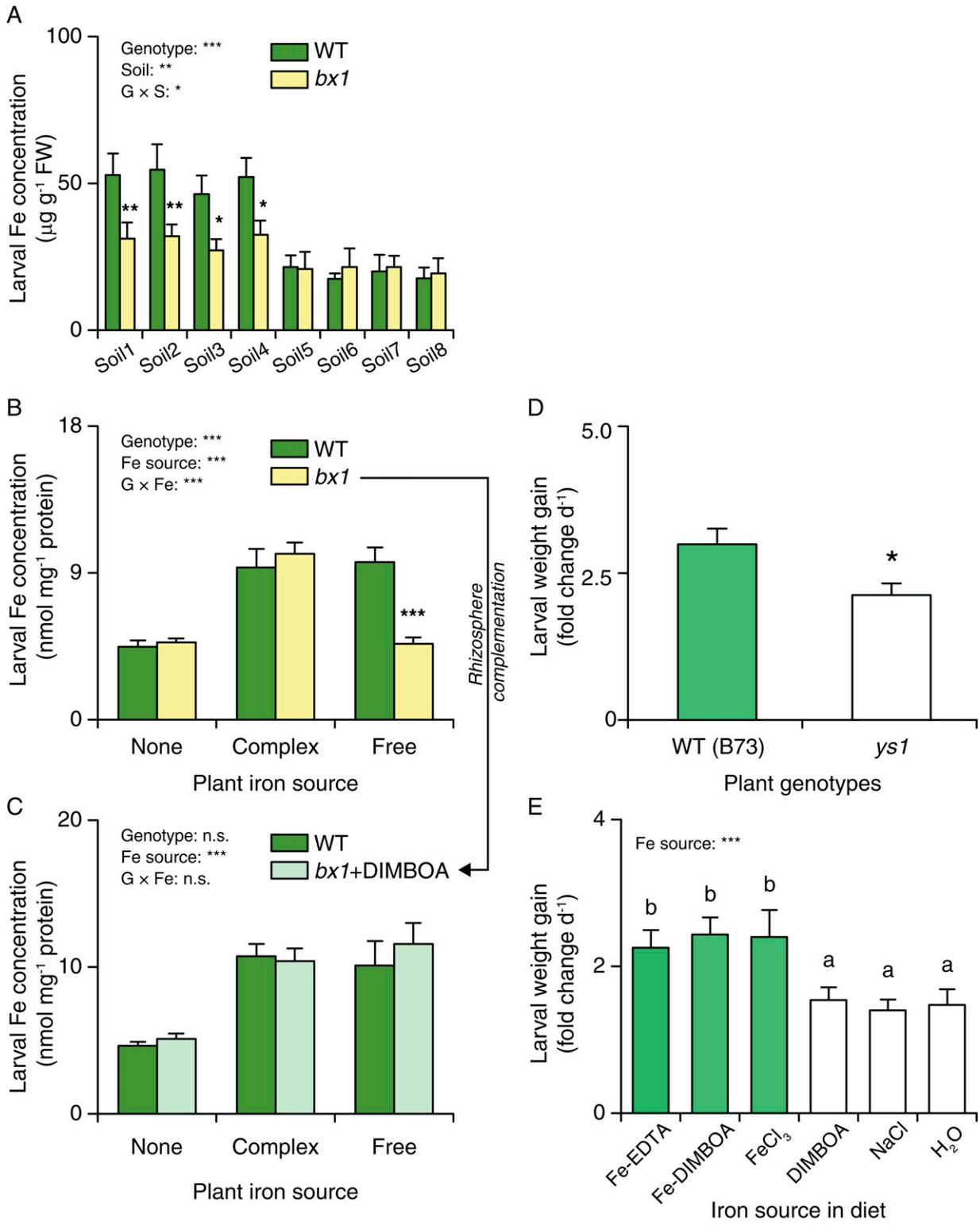

Fig. 6. Herbivore iron supply is associated with soil-dependent benzoxazinoid resistance. (*A*) Iron contents of *S. frugiperda* larvae feeding on WT and *bx1* plants grown in field soils (+SE, $n = 3$, with three to four individual larvae pooled per replicate). Soils 1 through 4 are anthrosols, and soils 5 through 8 are ferrosols. Twoway ANOVA results testing for genotype and soil effects are shown (*$P < 0.05$; **$P < 0.01$; ***$P < 0.001$). Asterisks indicate significant differences between genotypes within the same soil (pairwise comparisons through FDR-corrected LSMeans; *$P < 0.05$; **$P < 0.01$). (*B* and *C*) Iron contents of *S. frugiperda* larvae feeding on WT and *bx1* plants (*B*), with DIMBOA rhizosphere complementation (*C*) under different iron source treatments (+SE, $n = 5$, with three individual larvae pooled per replicate). "None" nutrient solutions received either NaCl or Na_2SO_4. "Complex" nutrient solutions received Fe-EDTA. "Free" nutrient solutions received $FeCl_3$ or $Fe_2(SO_4)_3$. For full results showing genotype effects of all individual nutrient solutions, refer to *SI Appendix*, Fig. S13. Two-way ANOVA results testing for genotype and iron source effects are shown (***$P < 0.001$). Asterisks indicate significant differences between genotypes within the same soil (pairwise comparisons through FDR-corrected LSMeans; ***$P < 0.001$). (*D*) Growth of *S. frugiperda* larvae feeding on B73 and *ys1* mutants (+SE, $n =$ 13 to 16). Note that the *ys1* mutant is in an undefined background. Asterisks indicate significant differences between plant genotypes (ANOVA; *$P < 0.05$). (*E*) Growth of *S. frugiperda* larvae feeding on the artificial diets supplemented with different iron sources (+SE, $n = 12$). Asterisks and letters indicate significant differences between genotypes or iron sources (one-way ANOVA followed by pairwise comparisons through FDR-corrected LSMeans; $P < 0.05$; ***$P < 0.001$).

noted that many other resistance factors apart from the ones measured here could contribute to the observed patterns. Nevertheless, the currently available data suggests that the direct effects of iron uptake on herbivore performance override potential indirect effects via root microbial communities or iron-dependent defense regulation.

Plant–herbivore interactions play an important role in shaping ecological communities and agricultural productivity (64, 65). Understanding the role of plant secondary metabolites as resistance factors is thus important for both fields. Our work shows that the suppressive effect of benzoxazinoids on fall armyworm growth, which likely contributes to plant resistance, depends on, and can even be reversed by, soil characteristics. In general, soil and plant chemistry interact to determine the outcome of plant–herbivore interactions above ground (22, 54). Through secondary metabolite multifunctionality, soil properties may determine plant and herbivore community composition even more strongly and dynamically than hitherto anticipated (66). From an agricultural point of view, the uncovered dependencies limit the use of benzoxazinoids as natural defenses against the fall armyworm, a global invasive pest that is currently threatening maize production in Africa and Asia. The finding that benzoxazinoids do not suppress the growth of the fall armyworm when growing in certain soils is of particular importance in the context of the rapidly expanding maize production in Asia, as it shows the limits of using a core innate defense mechanism to broadly protect agroecosystems from an important invasive pest.

Materials and Methods

Plants and Insects. The maize (*Zea mays* L.) genotypes B73 (referred to as WT), *bx1*/B73 (referred to as *bx1*) (33), W22, *bx1*/W22 (*bx1*::Ds), and *bx2*/W22 (*bx2*::Ds) (67) were used in this study. *ys1* mutants in an undefined genetic background (36, 46) were used to test the impacts of plant iron supply on larval performance. Fall armyworm *Spodoptera frugiperda* (J.E. Smith, 1791) larvae were reared on an artificial diet as described previously (68).

Plant and Herbivore Performance in Field Soils. To determine the impact of available soil nutrients on plant performance and herbivore resistance, we collected eight soils from different arable fields in Yixing, Jiangsu province, China (*SI Appendix*, Table S1). The soils were first air-dried and then individually passed through a 2-mm sieve, homogenized, and used to fill 200-mL pots (11-cm depth and 5-cm diameter). B73, *bx1*/B73, W22, *bx1*/W22, and *bx2*/W22 plants were then individually grown in these soils. Pots were randomly placed on a greenhouse table (26 °C ± 2 °C, 55% relative humidity, 14:10 h light/dark, 50,000 lm · m^{-2}) and rearranged weekly. Plants were watered once per week. A total of 16 d after planting, we measured the shoot dry weight, elemental composition ($n = 3$, with 3 to 4 plants pooled per replicate), and larval growth ($n = 10$) on each maize plant. Chlorophyll contents were determined using an SPAD-502 meter (Minolta Camera Co.).

Plant and Herbivore Performance in Nutrient Solutions. To assess the impact of different forms of iron on plant performance, a soil-free growth system was used as described previously (31). Briefly, B73 and *bx1* seeds were individually wrapped in two layers of paper. The paper rolls with the seeds were put in 200-mL pots (11-cm depth and 5-cm diameter). Pots were supplied with 40 mL Milli-Q water, covered with aluminum (Al) foil, and then placed in the greenhouse (26 °C ± 2 °C, 55% relative humidity, 14:10 h light/dark, 50,000 lm · m^{-2}). A period of 1 wk after the start of germination, the remaining seed shell was removed from the germinating seedlings to reduce the influence of residual iron in the endosperm. Plants were then grown in nutrient solutions containing complexed-iron (Fe-EDTA), free-iron [$FeCl_3$, $Fe_2(SO_4)_3$], or no-iron (NaCl, Na_2SO_4) sources. For a complete description of the nutrient solution, see ref. 31. The final concentrations of the different forms of iron in the solution were 250 μM Fe-EDTA, 250 μM $FeCl_3$, or 125 μM $Fe_2(SO_4)_3$. The respective Fe-free control solutions contained 750 μM NaCl or 375 μM Na_2SO_4 to control for effects of Cl^-, SO_4^{2-}, and Na^+ in the iron salt treatments. The pH of the nutrient solutions was adjusted to 5.5 using potassium hydroxide. All the chemicals were bought from Sigma (Sigma-Aldrich). A period of 3 wk after germination, we quantified the gene expression, primary and secondary metabolites of the youngest fully developed leaf ($n = 8$), and larval growth on each plant (n= 14 to 15).

To determine whether DIMBOA is sufficient to restore the resistance of *bx1* plants to those of WT plants, WT and *bx1* plants were treated as described in the previous paragraph. A period of 1 wk after germination, the plants were supplied with nutrient solutions containing Fe-EDTA, $FeCl_3$, or NaCl. The nutrient solution for the *bx1* mutants was complemented with 300 μg DIMBOA, which corresponds to physiological concentrations of DIMBOA that accumulate in the rhizosphere of B73 plants (31). The larval growth on each plant was then assessed as described in *Herbivore Growth and Damage Assays* ($n = 15$).

To investigate the connections between plant Fe acquisition and larval growth, B73 and *ys1* plants were treated as described above (n = 13 to 16). A period of 1 wk after germination, the plants were grown in nutrient solutions supplied with Fe-EDTA. A period of 3 wk after germination, larval growth on each plant was recorded.

Soil, Plant, and Herbivore Nutrient Analyses. To characterize nutrients in bulk field soil, soil samples were air-dried and then individually ground and passed through a 1-mm sieve. The available Fe, Mn, Ni, Cu, and Zn were extracted according to China Environmental Protection standards (HJ 804-2016). Briefly, 10.0 g soil sample was mixed with 20 mL extraction buffer (0.005 M diethylenetriaminepentaacetic acid [DTPA], 0.01 M $CaCl_2$, 0.1 M triethanolamine, pH = 7.3) and then shaken (180 rpm) for 2 h at 20 °C. DTPA is a strong chelator and has high affinity for metal cations. It can chelate and sequester free and weakly bond metal cations but not strongly chelated metal complexes and metal oxides in soil. After shaking, the mixture was centrifuged, supernatant was collected, and the concentrations of Fe, Mn, Ni, Cu, and Zn were determined by inductively coupled plasma mass spectrometry (ICP-MS) (NexION300X, PerkinElmer). The parameters used during the ICP-MS measurements were the following: radio frequency generator power output: 1,600 W; argon flows: plasma, 1.5 L · min^{-1}; nebulizer: 1.09 L · min^{-1}, kinetic energy discrimination gas: helium, at flow 3.5 mL · min^{-1}; optimization on masses of ^{9}Be, ^{24}Mg, ^{115}In, ^{238}U, ^{140}Ce; data acquisition: dwell time of 50 ms, three points per peak, acquisition time of 3 s. ^{57}Fe, ^{55}Mn, ^{60}Ni, ^{63}Cu, and ^{66}Zn were used as analytical masses to reduce interferences. A 40 μg · L^{-1} Rh solution as an internal standard in order to compensate any possible signal instability and a washing cycle of at least 30 s were settled between two subsequent samples with the aim to eliminate any memory effects. All reported data were blank corrected. In order to monitor constantly the overall accuracy level of the method, a blank was run up every eight samples. A standard reference material, certified reference material Cabbage, GBW10014 (GSB-5), prepared by the Institute of Geophysical and Geochemical Exploration of China, was run every 12 samples to determine the accuracy of the analytical methods. The mixed standard samples (PerkinElmer, catalog No. N9300233) from 1 μg · L^{-1} to 200 μg · L^{-1} were used to build a standard curve, with correlation coefficient (R^2) of each element being higher than 0.999. The absolute quantities of Fe, Mn, Ni, Cu, and Zn were calculated according to the standard curve.

Soil pH, NH_4^+, available P, S, Si, B, Mo, and exchangeable K^+, Na^+, Ca^{2+}, and Mg^{2+} were extracted and determined according to the China National Standard Methods. Briefly, soil pH was determined in a 2.5:1 water/soil suspension using a pH meter (LY/T1239-1999). NH_4^+ was measured using alkali hydrolysis diffusion (LY/T 1231-1999). Available P was determined by hydrochloric acid and ammonium fluoride (LY/T 1233-1999). Available S was extracted with calcium phosphate–acetic acid and quantified with the turbidimetric method using barium sulfate (LY/T 1265-1999). Available Si was extracted by sodium acetate and quantified by the silicon–molybdenum blue colorimetry (LY/T 1266-1999). Available B was extracted by boiled deionized water and determined by the azomethine-H spectrophotometric method (LY/T 1258-1999). Available Mo was extracted by acid–ammonium–oxalate and quantified by colorimetry using potassium thiocyanate (LY/T 1259-1999). Exchangeable K^+, Na^+, Ca^{2+}, and Mg^{2+} were extracted by ammonium acetate and determined by flame photometry (LY/T 1246-1999) and atomic absorption spectrophotometry (LY/T 1245-1999), respectively.

For plant micronutrient analyses, plant leaves were oven-dried. Three or four individual plants were pooled as one replicate. The samples were digested in 6 mL 15 M HNO_3 and 10 M H_2O_2 at 190 °C for 35 min with MARS 6 CLASSIC (CEM Corp.) as described (69). After digestion, the samples were dissolved in deionized water. The concentrations of Mg, Fe, Mn, Ni, Cu, and Zn were determined by ICP-MS as described in the previous paragraph. The concentrations of K, Ca, Na, P, Si, B, and Mo were quantified by the ICP–optical emission spectrometric method according to the China National Standard Method (GB/T 35871-2018).

For micronutrient analyses of fall armyworm larvae, three or four larvae were pooled together as one replicate. The elements were extracted and determined as described.

Herbivore Growth and Damage Assays. To assess the *S. frugiperda* growth on maize plants, individual starved and preweighted second-instar larvae were introduced into cylindrical mesh cages (1-cm height and 2.5-cm diameter). The cages were then clipped onto the leaves of maize plants (one cage per plant). The position of each cage was moved every day to provide sufficient food supply for the larvae. Larval weight was recorded 5 d after the start of the experiment. The remaining leaves were scanned, and the removed leaf area was quantified using Digimizer 4.6.1 (Digimizer).

Primary Metabolite Analyses. Soluble protein was extracted and quantified using a Bradford assay ($n = 8$) (70). Amino acids were hydrolyzed and quantified by ultra performance liquid chromatography–mass spectrometer (UHPLC-MS, Waters Corporation) according to a previously published protocol ($n = 8$) (71). Starch and soluble sugars (glucose, sucrose, and fructose) were extracted and quantified as described previously ($n = 8$) (72).

Secondary Metabolite Analyses. To quantify the influences of Fe forms on secondary metabolites, three maize plants were pooled, homogenized, and ground by liquid nitrogen ($n = 4$ pools per Fe treatment). A total of 70 mg ground samples was extracted in 700 μL acidified H_2O/MeOH (50:50 vol/vol; 0.1% formic acid) and then analyzed with an Acquity UHPLC system coupled to a G2-XS quadrupole time-of-flight (QTOF)-MS equipped with an electrospray source (Waters Corporation) as described (53). Briefly, compounds were separated on an Acquity BEH C18 column (2.1 × 50 mm inner diameter, 1.7-μm particle size). Water (0.1% formic acid) and acetonitrile (0.1% formic acid) were employed as mobile phases A and B. The elution profile was the following: 0 to 3.50 min, 99 to 72.5% A in B; 3.50 to 5.50 min, 72.5 to 50% B; 5.51 to 6.50 min 100% B; 6.51 to 7.51 min, 99% A in B. The flow rate was 0.4 mL/min. The column temperature was maintained at 40 °C, and the injection volume was 1 μL. The QTOF MS was operated in negative mode. The data were acquired over an *m/z* range of 50 to 1,200 with scans of 0.15 s at collision energy of 4 V and 0.2 s with a collision energy ramp from 10 to 40 V. The capillary and cone voltages were set to 2 kV and 20 V, respectively. The source temperature was maintained at 140 °C, the desolvation was 400 °C at 1,000 $L \cdot h^{-1}$, and cone gas flows were 50 L/h. Accurate mass measurements (<2 ppm) were obtained by infusing a solution of leucin encephalin at 200 ng/mL at a flow rate of 10 mL/min through the Lock Spray probe (Waters Corporation). The relative abundance of rutin was determined based on peak areas. The absolute quantities of chlorogenic acid, chlorogenic acid isomer, and maysin were determined using standard curves obtained from synthetic or purified standards.

Gene Expression Analyses. qRT-PCR was used to quantify gene expressions. Total RNA was isolated from maize leaves using the GeneJET Plant RNA Purification Kit (Thermo Fisher Scientific) following the manufacturer's instructions ($n = 8$). A total of 300 ng of each total RNA sample was reverse transcribed with SuperScript II Reverse Transcriptase (Invitrogen). The qRT-PCR assay was performed on the LightCycler 96 Instrument (Roche) using the KAPA SYBR FAST qPCR Master Mix (Kapa Biosystems). The maize actin gene *ZmActin* was used as an internal standard to normalize complementary DNA concentrations. The relative gene expression levels of target genes were calculated using the $2^{-\Delta\Delta Ct}$ method (73). The primers of all tested genes are provided in *SI Appendix*, Table S2.

Larval Iron Analyses. To determine iron concentrations in *S. frugiperda* larvae, three larvae were pooled and homogenized ($n = 5$ pools). Total protein of the larval lysates was extracted with 200 μL lysis buffer (20 mM Tris, 137 mM NaCl, 1% Triton X-100, 1% glycerol). The concentrations of extracted protein were quantified with a Bradford assay and then denatured using a described protocol (74). After denaturation, 50 μL supernatant was taken for iron measurements using the Iron Assay Kit (Sigma) following the manufacturer's instructions, with the modification that 25 μL saturated ammonium acetate was added and mixed to adjust the pH before measuring absorbance at 593 nm. The absolute quantities of iron were determined using standard curves made from pure $FeCl_3$ according to the manufacturer's instructions.

Larval Growth on Diets with Exogenous Iron Sources. To evaluate the direct effect of iron on *S. frugiperda* growth, we prepared the artificial diets containing different iron sources according to the methods as described in ref. 75, with some modifications. Briefly, 17 g agar was dissolved in 500 mL water at 50 °C and mixed with 5 g dried leaf material of *bx1* plants, 25 g casein, 23 g sucrose, 12 g yeast extract, 9 g Wesson salt mixture, 3.5 g ascorbic acid, 2.5 g cholesterol, 1.5 g sorbic acid, 5 mL raw linseed oil, 1.5 mL formalin, and 9 mL vitamin mixture (100 mg nicotinic acid, 500 mg riboflavin, 233.5 mg thiamine, 233.5 mg pyridoxine, 233.5 mg folic acid, and 20 mg $\cdot L^{-1}$ biotin in water). Fe-EDTA, Fe(III)(DIMBOA)$_3$, $FeCl_3$, DIMBOA, NaCl, or H_2O was then added to the diet at a final concentration of 50 μM, which corresponds to the physiological concentration in maize xylem sap (31). The produced diet was aliquoted into Solo cups. One starved and preweighted second-instar larva was individually introduced into the Solo cups. Diets were replaced every other day. Larval weight was recorded 5 d after the start of the experiment ($n = 12$).

Statistical Analyses. Larval growth, leaf damage, gene expression, and metabolite data were analyzed by ANOVA followed by pairwise or multiple comparisons of least squares means (LSMeans), which were corrected using the false discovery rate (FDR) method (76). The tested factors and interactions are provided directly in the figures. Normality was verified by inspecting residuals, and homogeneity of variance was tested through the Shapiro–Wilk tests using the "plotresid" function of the R package "RVAideMemoire" (77). Datasets that did not fit assumptions (Figs. 2 *B* and *C*, 3, 5 *A*, *E*, and *F*, and 6 *B* and *E* and *SI Appendix*, S4 *C* and *L*, S8, and S10 *A*, *E*, and *F*) were natural log–transformed. For the redundancy analysis, raw data were first scaled with the "scale" function in R. PCAs were then performed with the "MVA" function of the "RVAideMemoire" package and the "rda" function of the "vegan" package (77, 78). All statistical analyses were conducted with R 3.4.4 (R Foundation for Statistical Computing) using the packages "car," "emmeans," and "RVAideMemoire" (77–80).

Accession Numbers. The sequence data of maize genes can be found in the MaizeGDB database under the following accession numbers *ZmActin* (GRMZM2G126010), *ZmMPI* (GRMZM2G028393), *ZmRIP2* (GRMZM2G119705), *ZmRPI* (GRMZM2G035599), *ZmIDI4* (GRMZM2G067265), *ZmNAS3* (GRMZM2G478568), *ZmDMAS1* (GRMZM2G060952), *ZmTOM2* (GRMZM5G877788), *ZmYS1* (GRMZM2G156599), *ZmNRAMP1* (GRMZM2G178190) and *ZmIRO2* (GRMZM2G057413).

Data Availability. All the raw data supporting the findings of this study can be downloaded from the DRYAD repository (doi: 10.5061/dryad.0k6djhb15).

ACKNOWLEDGMENTS. We thank Professor Nicolaus von Wirén from Institut für Pflanzengenetik und Kulturpflanzenforschung Gatersleben for sharing the *ys1* mutants and Dr. Xianwen Zhang from Zhejiang University for propagating the seeds. This work was supported by the National Natural Science Foundation of China (41721001, 42007029, and 42090061), the Young Elite Scientists Sponsorship Program by the China Association for Science and Technology (2020QNRC002), the Interfaculty Research Collaboration "One Health" of the University of Bern, the Fundamental Research Funds for the Central Universities (2020QNA6009), and the Schweizerischer Nationalfonds zur Förderung der Wissenschaftlichen Forschung (310030_189071).

1. S. C. Farina, E. A. Kane, L. P. Hernandez, Multifunctional structures and multistructural functions: Integration in the evolution of biomechanical systems. *Integr. Comp. Biol.* **59**, 338–345 (2019).
2. D. S. Tawfik, Messy biology and the origins of evolutionary innovations. *Nat. Chem. Biol.* **6**, 692–696 (2010).
3. R. J. Greenspan, The flexible genome. *Nat. Rev. Genet.* **2**, 383–387 (2001).
4. E. H. Neilson, J. Q. D. Goodger, I. E. Woodrow, B. L. Møller, Plant chemical defense: At what cost? *Trends Plant Sci.* **18**, 250–258 (2013).
5. N. R. Friedman *et al.*, Evolution of a multifunctional trait: Shared effects of foraging ecology and thermoregulation on beak morphology, with consequences for song evolution. *Proc. Biol. Sci.* **286**, 20192474 (2019).
6. B. Li *et al.*, Convergent evolution of a metabolic switch between aphid and caterpillar resistance in cereals. *Sci. Adv.* **4**, eaat6797 (2018).
7. R. Li *et al.*, Prioritizing plant defence over growth through WRKY regulation facilitates infestation by non-target herbivores. *eLife* **4**, e04805 (2015).
8. T. Hartmann, From waste products to ecochemicals: Fifty years research of plant secondary metabolism. *Phytochemistry* **68**, 2831–2846 (2007).
9. A. Mithöfer, W. Boland, Plant defense against herbivores: Chemical aspects. *Annu. Rev. Plant Biol.* **63**, 431–450 (2012).
10. N. K. Clay, A. M. Adio, C. Denoux, G. Jander, F. M. Ausubel, Glucosinolate metabolites required for an Arabidopsis innate immune response. *Science* **323**, 95–101 (2009).
11. G. Agati, M. Tattini, Multiple functional roles of flavonoids in photoprotection. *New Phytol.* **186**, 786–793 (2010).
12. M. Huang *et al.*, The major volatile organic compound emitted from *Arabidopsis thaliana* flowers, the sesquiterpene (E)-β-caryophyllene, is a defense against a bacterial pathogen. *New Phytol.* **193**, 997–1008 (2012).
13. N. B. Schmid *et al.*, Feruloyl-CoA 6'-Hydroxylase1-dependent coumarins mediate iron acquisition from alkaline substrates in Arabidopsis. *Plant Physiol.* **164**, 160–172 (2014).

14. E. Soubeyrand *et al.*, The peroxidative cleavage of kaempferol contributes to the biosynthesis of the benzenoid moiety of ubiquinone in plants. *Plant Cell* **30**, 2910–2921 (2018).
15. M. Erb, D. J. Kliebenstein, Plant secondary metabolites as defenses, regulators, and primary metabolites: The blurred functional trichotomy. *Plant Physiol.* **184**, 39–52 (2020).
16. E. Pichersky, R. A. Raguso, Why do plants produce so many terpenoid compounds? *New Phytol.* **220**, 692–702 (2018).
17. D. J. Ballhorn, A. Pietrowski, R. Lieberei, Direct trade-off between cyanogenesis and resistance to a fungal pathogen in lima bean (*Phaseolus lunatus* L.). *J. Ecol.* **98**, 226–236 (2010).
18. D. Baek, H. J. Chun, D. J. Yun, M. C. Kim, Cross-talk between phosphate starvation and other environmental stress signaling pathways in plants. *Mol. Cells* **40**, 697–705 (2017).
19. L. A. J. Mur, C. Simpson, A. Kumari, A. K. Gupta, K. J. Gupta, Moving nitrogen to the centre of plant defence against pathogens. *Ann. Bot.* **119**, 703–709 (2017).
20. A. Martínez-Medina, S. C. M. Van Wees, C. M. J. Pieterse, Airborne signals from Trichoderma fungi stimulate iron uptake responses in roots resulting in priming of jasmonic acid-dependent defences in shoots of *Arabidopsis thaliana* and *Solanum lycopersicum*. *Plant Cell Environ.* **40**, 2691–2705 (2017).
21. I. A. Stringlis *et al.*, MYB72-dependent coumarin exudation shapes root microbiome assembly to promote plant health. *Proc. Natl. Acad. Sci. U.S.A.* **115**, E5213–E5222 (2018).
22. D. Debona, F. A. Rodrigues, L. E. Datnoff, Silicon's role in abiotic and biotic plant stresses. *Annu. Rev. Phytopathol.* **55**, 85–107 (2017).
23. J. D. Schade, M. Kyle, S. E. Hobbie, W. F. Fagan, J. J. Elser, Stoichiometric tracking of soil nutrients by a desert insect herbivore. *Ecol. Lett.* **6**, 96–101 (2003).
24. E. R. D. Moise, J. N. McNeil, S. E. Hartley, H. A. L. Henry, Plant silicon effects on insect feeding dynamics are influenced by plant nitrogen availability. *Entomol. Exp. Appl.* **167**, 91–97 (2019).
25. M. Frey, K. Schullehner, R. Dick, A. Fiesselmann, A. Gierl, Benzoxazinoid biosynthesis, a model for evolution of secondary metabolic pathways in plants. *Phytochemistry* **70**, 1645–1651 (2009).
26. H. M. Niemeyer, Hydroxamic acids derived from 2-hydroxy-2H-1,4-benzoxazin-3(4H)-one: Key defense chemicals of cereals. *J. Agric. Food Chem.* **57**, 1677–1696 (2009).
27. S. Ahmad *et al.*, Benzoxazinoid metabolites regulate innate immunity against aphids and fungi in maize. *Plant Physiol.* **157**, 317–327 (2011).
28. L. N. Meihls *et al.*, Natural variation in maize aphid resistance is associated with 2,4-dihydroxy-7-methoxy-1,4-benzoxazin-3-one glucoside methyltransferase activity. *Plant Cell* **25**, 2341–2355 (2013).
29. C. A. M. Robert *et al.*, A specialist root herbivore exploits defensive metabolites to locate nutritious tissues. *Ecol. Lett.* **15**, 55–64 (2012).
30. L. Bigler, A. Baumeler, C. Werner, M. Hesse, Detection of noncovalent complexes of hydroxamic-acid derivatives by means of electrospray mass spectrometry. *Helv. Chim. Acta* **79**, 1701–1709 (1996).
31. L. Hu *et al.*, Plant iron acquisition strategy exploited by an insect herbivore. *Science* **361**, 694–697 (2018).
32. G. Glauser *et al.*, Induction and detoxification of maize 1,4-benzoxazin-3-ones by insect herbivores. *Plant J.* **68**, 901–911 (2011).
33. D. Maag *et al.*, Highly localized and persistent induction of *Bx1*-dependent herbivore resistance factors in maize. *Plant J.* **88**, 976–991 (2016).
34. C. Poschenrieder, R. P. Tolrà, J. Barceló, A role for cyclic hydroxamates in aluminium resistance in maize? *J. Inorg. Biochem.* **99**, 1830–1836 (2005).
35. C. Curie *et al.*, Maize *yellow stripe1* encodes a membrane protein directly involved in Fe(III) uptake. *Nature* **409**, 346–349 (2001).
36. S. N. Chorianopoulou, Y. I. Saridis, M. Dimou, P. Katinakis, D. L. Bouranis, Arbuscular mycorrhizal symbiosis alters the expression patterns of three key iron homeostasis genes, *ZmNAS1, ZmNAS3*, and *ZmYS1*, in S deprived maize plants. *Front Plant Sci* **6**, 257 (2015).
37. T. Nozoye, H. Nakanishi, N. K. Nishizawa, Characterizing the crucial components of iron homeostasis in the maize mutants *ys1* and *ys3*. *PLoS One* **8**, e62567 (2013).
38. M. Jahangir, I. B. Abdel-Farid, Y. H. Choi, R. Verpoorte, Metal ion-inducing metabolite accumulation in *Brassica rapa*. *J. Plant Physiol.* **165**, 1429–1437 (2008).
39. G. Vigani *et al.*, Knocking down mitochondrial iron transporter (MIT) reprograms primary and secondary metabolism in rice plants. *J. Exp. Bot.* **67**, 1357–1368 (2016).
40. J. H. Herlihy, T. A. Long, J. M. McDowell, Iron homeostasis and plant immune responses: Recent insights and translational implications. *J. Biol. Chem.* **295**, 13444–13457 (2020).
41. B. R. Wiseman, R. C. Gueldner, R. E. Lynch, R. F. Severson, Biochemical activity of centipedegrass against fall armyworm larvae. *J. Chem. Ecol.* **16**, 2677–2690 (1990).
42. T. R. F. B. Silva *et al.*, Effect of the flavonoid rutin on the biology of *Spodoptera frugiperda* (Lepidoptera: Noctuidae). *Acta Sci. Agron.* **38**, 165–170 (2016).
43. B. R. Wiseman, M. E. Snook, D. J. Isenhour, J. A. Mihm, N. W. Widstrom, Relationship between growth of corn earworm and fall armyworm larvae (Lepidoptera: Noctuidae) and maysin concentration in corn silks. *J. Econ. Entomol.* **85**, 2473–2477 (1992).
44. M. C. Tamayo, M. Rufat, J. M. Bravo, B. San Segundo, Accumulation of a maize proteinase inhibitor in response to wounding and insect feeding, and characterization of its activity toward digestive proteinases of *Spodoptera littoralis* larvae. *Planta* **211**, 62–71 (2000).
45. W. P. Chuang *et al.*, Caterpillar attack triggers accumulation of the toxic maize protein RIP2. *New Phytol.* **201**, 928–939 (2014).
46. N. Von Wiren, S. Mori, H. Marschner, V. Romheld, Iron inefficiency in maize mutant ys1 (*Zea mays* L cv yellow-stripe) is caused by a defect in uptake of iron phytosiderophores. *Plant Physiol.* **106**, 71–77 (1994).
47. L. Sack, T. N. Buckley, Trait multi-functionality in plant stress response. *Integr. Comp. Biol.* **60**, 98–112 (2020).
48. S. Zhou, A. Richter, G. Jander, Beyond defense: Multiple functions of benzoxazinoids in maize metabolism. *Plant Cell Physiol.* **59**, 1528–1537 (2018).
49. D. J. Kliebenstein, Plant nutrient acquisition entices herbivore. *Science* **361**, 642–643 (2018).
50. F. C. Wouters, B. Blanchette, J. Gershenzon, D. G. Vassão, Plant defense and herbivore counter-defense: Benzoxazinoids and insect herbivores. *Phytochem. Rev.* **15**, 1127–1151 (2016).
51. F. C. Wouters *et al.*, Reglucosylation of the benzoxazinoid DIMBOA with inversion of stereochemical configuration is a detoxification strategy in lepidopteran herbivores. *Angew. Chem. Int. Ed. Engl.* **53**, 11320–11324 (2014).
52. A. Köhler *et al.*, Within-plant distribution of 1,4-benzoxazin-3-ones contributes to herbivore niche differentiation in maize. *Plant Cell Environ.* **38**, 1081–1093 (2015).
53. L. Hu *et al.*, Root exudate metabolites drive plant-soil feedbacks on growth and defense by shaping the rhizosphere microbiota. *Nat. Commun.* **9**, 2738 (2018).
54. Y. Lou, I. T. Baldwin, Nitrogen supply influences herbivore-induced direct and indirect defenses and transcriptional responses in *Nicotiana attenuata*. *Plant Physiol.* **135**, 496–506 (2004).
55. T. J. Massad, L. A. Dyer, G. Vega C, Costs of defense and a test of the carbon-nutrient balance and growth-differentiation balance hypotheses for two co-occurring classes of plant defense. *PLoS One* **7**, e47554 (2012).
56. W. C. Wetzel, H. M. Kharouba, M. Robinson, M. Holyoak, R. Karban, Variability in plant nutrients reduces insect herbivore performance. *Nature* **539**, 425–427 (2016).
57. C. Cabot *et al.*, A role for zinc in plant defense against pathogens and herbivores. *Front Plant Sci* **10**, 1171 (2019).
58. E. H. Verbon *et al.*, Iron and immunity. *Annu. Rev. Phytopathol.* **55**, 355–375 (2017).
59. S. N. Johnson *et al.*, Silicon-induced root nodulation and synthesis of essential amino acids in a legume is associated with higher herbivore abundance. *Funct. Ecol.* **31**, 1903–1909 (2017).
60. F. P. Massey, S. E. Hartley, Physical defences wear you down: Progressive and irreversible impacts of silica on insect herbivores. *J. Anim. Ecol.* **78**, 281–291 (2009).
61. S. N. Johnson *et al.*, Siliceous and non-nutritious: Nitrogen limitation increases anti-herbivore silicon defences in a model grass. *J. Ecol.* 10.1111/1365-2745.13755. (2021).
62. E. N. Kudjordjie, R. Sapkota, S. K. Steffensen, I. S. Fomsgaard, M. Nicolaisen, Maize synthesized benzoxazinoids affect the host associated microbiome. *Microbiome* **7**, 59 (2019).
63. T. E. A. Cotton *et al.*, Metabolic regulation of the maize rhizobiome by benzoxazinoids. *ISME J.* **13**, 1647–1658 (2019).
64. E. S. Bakker, M. E. Ritchie, H. Olff, D. G. Milchunas, J. M. Knops, Herbivore impact on grassland plant diversity depends on habitat productivity and herbivore size. *Ecol. Lett.* **9**, 780–788 (2006).
65. T. Ohgushi, Eco-evolutionary dynamics of plant-herbivore communities: Incorporating plant phenotypic plasticity. *Curr. Opin. Insect Sci.* **14**, 40–45 (2016).
66. D. A. Wardle *et al.*, Ecological linkages between aboveground and belowground biota. *Science* **304**, 1629–1633 (2004).
67. V. Tzin *et al.*, Dynamic maize responses to aphid feeding are revealed by a time series of transcriptomic and metabolomic assays. *Plant Physiol.* **169**, 1727–1743 (2015).
68. D. Maag *et al.*, 3-β-D-Glucopyranosyl-6-methoxy-2-benzoxazolinone (MBOA-*N*-Glc) is an insect detoxification product of maize 1,4-benzoxazin-3-ones. *Phytochemistry* **102**, 97–105 (2014).
69. H. Yuan *et al.*, Warming facilitates microbial reduction and release of arsenic in flooded paddy soil and arsenic accumulation in rice grains. *J. Hazard. Mater.* **408**, 124913 (2021).
70. N. M. van Dam, M. Horn, M. Mares, I. T. Baldwin, Ontogeny constrains systemic protease inhibitor response in *Nicotiana attenuata*. *J. Chem. Ecol.* **27**, 547–568 (2001).
71. T. Docimo *et al.*, The first step in the biosynthesis of cocaine in *Erythroxylum coca*: The characterization of arginine and ornithine decarboxylases. *Plant Mol. Biol.* **78**, 599–615 (2012).
72. R. A. R. Machado *et al.*, Leaf-herbivore attack reduces carbon reserves and regrowth from the roots via jasmonate and auxin signaling. *New Phytol.* **200**, 1234–1246 (2013).
73. M. L. Wong, J. F. Medrano, Real-time PCR for mRNA quantitation. *Biotechniques* **39**, 75–85 (2005).
74. F. Missirlis *et al.*, Characterization of mitochondrial ferritin in *Drosophila*. *Proc. Natl. Acad. Sci. U.S.A.* **103**, 5893–5898 (2006).
75. R. A. R. Machado, C. C. M. Arce, A. P. Ferrieri, I. T. Baldwin, M. Erb, Jasmonate-dependent depletion of soluble sugars compromises plant resistance to *Manduca sexta*. *New Phytol.* **207**, 91–105 (2015).
76. Y. Benjamini, Y. Hochberg, Controlling the false discovery rate: A practical and powerful approach to multiple testing. *J. R. Stat. Soc. Series B Stat. Methodol.* **57**, 289–300 (1995).
77. M. R. Herve, RVAideMemoire: Testing and plotting procedures for biostatistics. https://cran.r-project.org/web/packages/RVAideMemoire/index.html. Accessed 28 June 2021.
78. J. Oksanen *et al.*, Vegan: Community ecology package. R package version 2.0-10. CRAN.R-project.org/package=vegan. Accessed 28 November 2020.
79. D. Bates, M. Machler, B. M. Bolker, S. C. Walker, Fitting linear mixed-effects models using lme4. *J. Stat. Softw.* **67**, 1–48 (2015).
80. R. V. Lenth, Least-squares means: The R Package lsmeans. *J. Stat. Softw.* **69**, 1–33 (2016).